Use of Analog Two-Phase Relative Permeability Data to estimate drainage CO_2/Brine Relative Permeability Curves.

Josephina Schembre-McCabe*, *Morteza* Akbarabadi, *Jon* Burger, *Michael* Rauschhuber, *Will* Richardson.

Chevron Technical Center, Chevron, Houston, Texas

Abstract. Relative permeability is a crucial parameter for modeling multiphase flow in porous media. However, experimental data on CO_2/brine relative permeability are scarce and often inconsistent due to the experimental challenges such as solubility and water evaporation. As a result, most of the available CO_2/brine relative permeability data cover the early stages of the relative permeability curve, because high gas relative permeabilities during the drainage process are difficult to achieve. In this study, we propose a novel approach to estimate drainage CO_2/brine relative permeability curve from analog fluids and available CO_2/brine relative permeability data. Finally, we integrate pore scale modeling simulations to gain additional insight and propose a workflow to use the analog fluid relative permeability curves to supplement CO_2/brine relative permeability curves. We validate our approach by systematically comparing CO_2/brine relative permeability curves with other fluid-pairs and demonstrate that we can capture the key features and trends of the CO_2/brine relative permeability behavior. Our method provides a simple and promising workflow to use routine fluid systems to predict CO_2/brine relative permeability in which experimental measurements are more challenging.

1 Introduction

Understanding the behavior of fluids within porous media is essential for reservoir engineering. Relative permeability is considered as a key factor in accurately modeling how multiple fluid phases, such as gas (e.g., CO_2) and liquid, flow through these porous structures. CO_2/brine relative permeability has been a subject of increasing importance given its implications for carbon sequestration and enhanced oil recovery processes.

The scarcity and inconsistency of experimental data on CO_2/brine relative permeability pose significant challenges for researchers and engineers. These challenges are primarily due to the nature of the experiments, which are often plagued by issues like solubility of CO_2 in the brine due to changes in equilibrium, as well as the evaporation of water during the process. Consequently, the available data tend to focus predominantly on the initial segments of the relative permeability curve. Achieving and measuring high gas relative permeabilities, especially during the drainage phase, remains a challenging task limiting our understanding of the relative permeability for a broad range of saturations. Core-scale experimental studies have been pivotal in understanding the relative permeability properties of CO_2/brine systems.

Various experimental studies have been published, detailing drainage CO_2/brine relative permeability values under diverse conditions [1-20]. It is important to acknowledge the challenges in maintaining CO_2/brine equilibrium due to temperature and pressure variations, along with other uncertainties in core flooding experiments. These factors make it difficult to achieve high CO_2 flow rates during the drainage process, resulting in scarce data on CO_2 relative permeability at lower brine saturations, nearing irreducible levels, in the literature. Conversely, there is an abundance of relative permeability data for various field, analog rock samples and fluid pairs (e.g., nitrogen/brine, mineral oil/brine, nitrogen/mineral oil) in the literature [14,22-28] and in companies repositories.

In this analysis, we compare various fluid pair systems in a narrow set of sandstone rocks published in the literature [1,7,14,17,18,20,23] under an uncertainty-based framework [29,30]; in this approach we look at total mobility and displacement efficiency while observing capillary numbers and mobility ratios to address the following questions:

- Can we employ existent data derived for other fluid pair to forecast the entire CO_2/brine drainage relative permeability curve for samples with similar properties?
- Is it feasible to represent CO_2/brine drainage relative permeability curve by performing simpler and faster experiments?

To answer these questions, we propose a workflow and based on our observations provide guidelines for further studies.

* Corresponding author: jschembremccabe@chevron.com

2 Background

2.1. Source of uncertainties in CO_2/Brine studies

We take the framework laid out by Kamath *et al.* [29] to gauge uncertainties in a CCUS project by adjusting to the objectives of the project (injection and storage) and bracket the analysis based on the following sources of uncertainty,

Sample-related uncertainty: sampling focuses on capturing the variability of the reservoir target, and testing in this stage is based on solid sampling and characterization program. For 'standard testing' in this stage, we should focus on N_2-brine or N_2-mineral oil endpoint testing (for injectivity) and CCI for various initial water saturation for trapped gas.

Process-related uncertainty: a sub-set of samples should be used to test the effects of various factors, type of test, cleaning/treating method, capillary number, interfacial tension, viscosity ratio, reservoir conditions, etc. This is important to assess the impact of experimental protocols, which is ubiquitous in projects with a long history and when working with analog data. Figure 1 shows the ranges of viscosity ratio and IFT ranges used in most CO_2/Brine drainage relative permeability, the numbers indicate the reference in this work. Some authors have done some work on looking at the effects of IFT, viscosity ratio and/or both[1]. We will go into more detail on the effects of each factor in the next session.

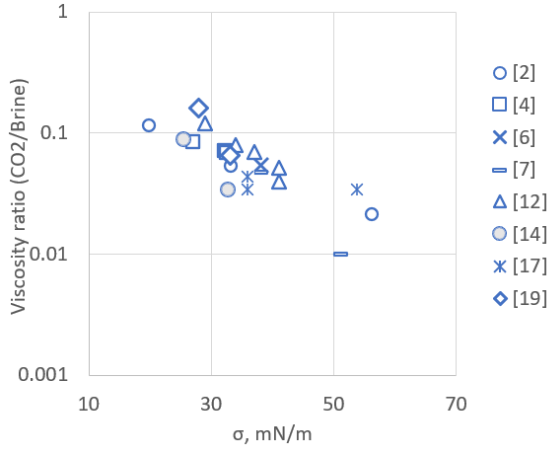

Fig. 1. Viscosity ratio and IFT ranges the literature related to CO_2/Brine drainage relative permeability.

Experimental uncertainties: while design of the protocols attempt to minimize this type of uncertainties throughout the whole experimental process, we can still have them due to various factors. Examples of sources of experimental uncertainty are cleaning protocols, non-expected rock-fluid interactions, channeling, end-effects, incomplete equilibration of fluids, etc.

Subjective uncertainty: while it is difficult to gauge, we aim to reduce this uncertainty by taking a thorough review of assumptions made during designing sampling strategy and gauging the influence of various mechanisms.

Following this workflow, we focus on published studies performed on sandstones within a limited range of porosity (17-25%) and air permeability (50-800 mD), and excluded work that indicated effects of heterogeneity. The permeability range considered for this subset is larger than we would generally include as a rock type in the uncertainty analysis. We are expanding the window of viscosity ratio and IFT in Figure 1 by including other fluid pairs generally used in the industry (Figure 2). In this study, process and experimental uncertainty are our main concern followed by the subjective uncertainty.

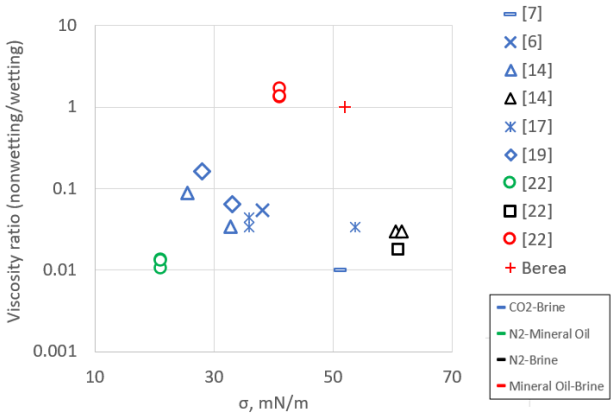

Fig. 2. Viscosity ratio and IFT ranges considered in this study.

Figure 3 shows the relative permeability for these studies, colors denote fluid-pairs. Some observations in Figure 3: (a) the brine (wetting) relative permeability for the CO_2/brine pair (in blue) shows larger spread than other pairs, (b) the CO_2 (non-wetting phase) relative permeability shows a narrow range with other fluid pairs but reaching a lower non-wetting phase saturation (they generally don't extend past $S_{nw} \sim 55\%$). This observation has been discussed in the literature [8, 20, 31,32] and part of it is due to a combination of low CO_2 viscosity and the difficulty in measuring the relative permeability when equilibrated fluids are needed at high flow rates for an extended period.

[1] Values of IFT for some of this work was estimated from experimental conditions reported by the authors.

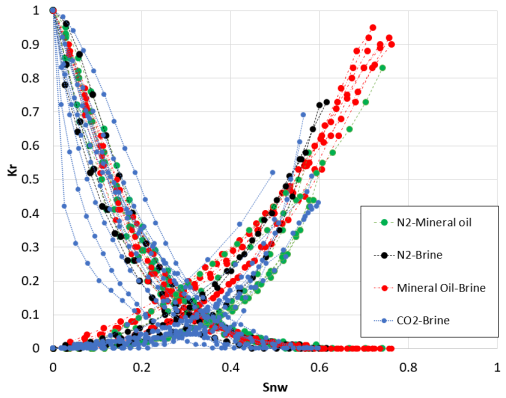

Fig. 3. Wetting and non-wetting relative permeability for different fluid pairs in the literature reviewed.

2.2. Capillary number

This research compares selected parameters which describe fluid flow and rock properties across the different fluid/rock systems. The ratio of viscous to interfacial forces is defined for each rock/fluid system with the capillary number presented in Saffman and Taylor [31],

$$N_c = u\mu/\sigma \qquad (1)$$

Figure 4 compares relative permeability endpoints for the non-wetting phase shown in Figure 3 as a function of the capillary number. Most of these data show capillary dominated flow. Data for the CO_2/brine pair shows even lower capillary numbers, which is a product of a relatively high IFT and low rates in the experiments. However, during CO_2 injection operations we will need endpoints for higher capillary numbers to cover the saturations reached during injection near the wellsite.

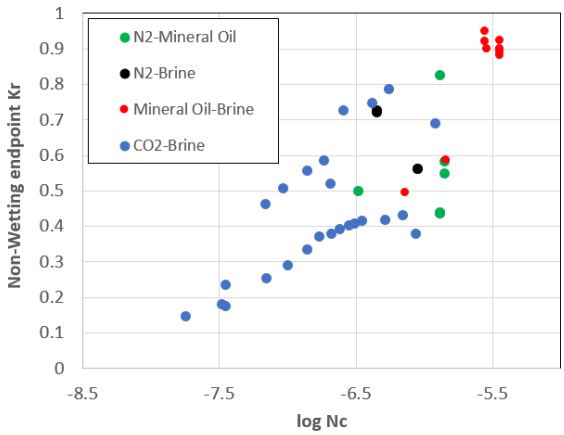

Fig. 4. Non-wetting relative permeability endpoint as a function of experimental capillary number.

Phase- and Total- Mobility

Total mobility is a measure of injectivity, we first gauge the uncertainty associated with injectivity by estimating the mobility for any given two-phase coreflood experiment by applying,

$$\lambda_T(S_{p1}) = \lambda_{p1}(S_{p1}) + \lambda_{p2}(S_{p1}) \qquad (2)$$

where the mobilities of injected and displaced (λ_{pdisp}) fluid are defined by

$$\lambda_{pi}(S_{p1}) = k_{rpi}(S_{p1})/\mu_p \qquad (3)$$

Figure 5 shows the total mobility for the reviewed data in the literature, colors indicate the fluid pair, in this plot we use the reported experimental viscosity. This plot shows lowest total mobility for mineral oil/brine experiments compared to the other fluid pairs. A relatively low total mobility can only be achieved if the mobility of each phase is low; and a high total mobility can be achieved if either one or both phases are high. As we go towards increasing non-wetting phase, which is gas in two of the fluid pairs, the gas mobility moves this injectivity upwards.

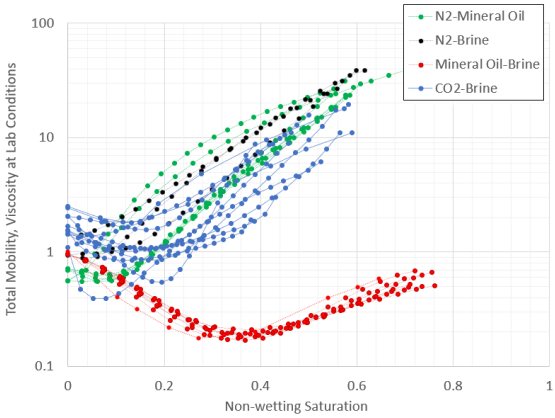

Fig. 5. Total mobility as a function of non-wetting phase saturation (injected phase). Total mobility is calculated using viscosities in experimental conditions.

2.3 Fractional Flow

The fractional flow equation [34] is useful to understand the combined effect of viscosity and relative permeability in displacement, the fractional flow assumes linear one-dimension, incompressible, immiscible fluids, and can be written as [35]

$$f_{p1} = \frac{1}{1+\frac{k_{rp1}\mu_2}{k_{rp2}\mu_1}} \qquad (4)$$

For consistency across the study, we define *p1* in equations 2, 3 and 4 as the phase being injected. Figure 6 shows the fractional flow for the data reviewed, using the experimental viscosities. As in the case of injectivity, the CO_2/brine pair is between the mineral oil/brine and N_2/brine; N_2/brine and N_2/mineral oil are in the same range. As a side note, when we plot data as total mobility or as fractional curve, we have a combination of the effects of variability of the plug and experimental protocols; the next section describes a brief exercise to differentiate one effect from the other.

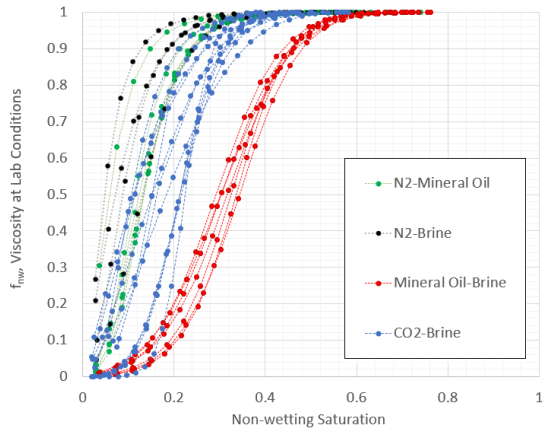

Fig. 6. Non-wetting fractional flow as a function of non-wetting saturation. (Fractional flow calculated using viscosities at experimental conditions).

3. Geological and Process related uncertainty

3.1 Digital Rock Analysis.

When looking at these studies, we are facing the issue that geological and process uncertainty are intertwined; the fluid viscosity ratio ranged between 0.02 and 1, and IFT between 20 and 60 mN/m (approximately). While these factors certainly affect the relative permeability, we could use digital rock physics to see how they move the uncertainty band while we look at them under the framework.

Digital rock simulations were done using lattice Boltzmann on high resolution image (2 µm/voxel) of a Bentheimer sandstone sample, with a porosity of 24% and permeability 2,400 mD. Three numerical experiments were done with non-wetting to wetting phase viscosity ratios of 0.02, 0.1 and 1 while keeping the capillary number constant at 10^{-5} (see Figure 7). These viscosity ratios are representative of the studies reviewed in this work. A similar trend in the relative has been captured experimentally [2, 19] and using digital rock physics [36, 37].

In the last section, we use the experimental viscosities to look at the effect of experimental conditions on the mobility and fractional flow. We follow up with the exercise of showing how these sets of relative permeability in Figure 7, that have been obtained with different mobility ratios (process uncertainty), affect output, total mobility, and fractional flow. These are shown in Figure 8 and Figure 9, respectively, for the case of using the same non-wetting to wetting phase viscosity ratio (0.1) in computing each curve. Use of the frontal advance equation (Figure 10), is another way of using fractional flow information in Figure 9 to identify, rank and quantify effects of experimental conditions on remaining fluid saturation [29].

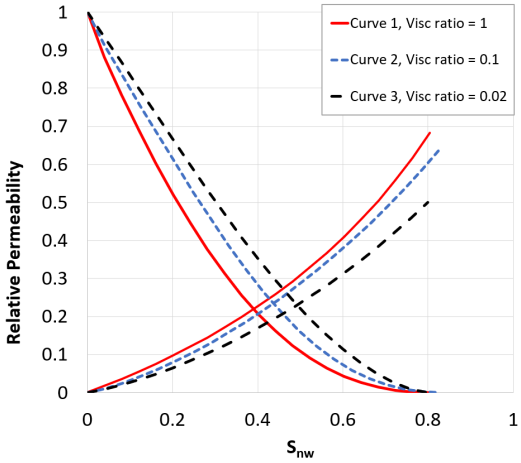

Fig. 7. Wetting and non-wetting relative permeability for different non-wetting to wetting phase viscosity ratios at constant capillary number.

This exercise illustrates the effects of process (in this case, viscosity ratio) when the uncertainty due to contribution of the variability in the samples is removed from the pool of data to be analyzed. Figure 8, Figure 9, and Figure 10 show that the uncertainty range is small compared to what we observe in the literature, if we only take viscosity ratio as the variable. We did not probe other factors such as IFT and/or capillary number but based on the range of results obtained by other authors [36] on Berea Sandstone, we expect to see similar limited effects in the uncertainty band for the considered range. Nonetheless, this should be investigated further.

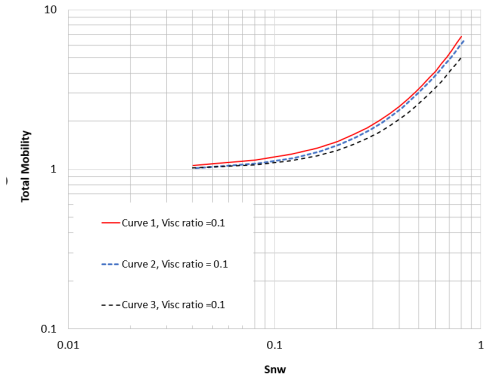

Fig. 8. Total mobility as a function of non-wetting phase saturation (injected phase). Total mobility is calculated using relative permeability in Figure 7 with viscosity ratio of 0.1.

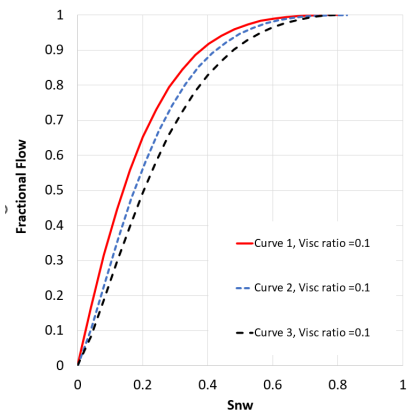

Fig. 9. Fractional flow of the non-wetting phase calculated using relative permeability in Figure 7 with viscosity ratio of 0.1.

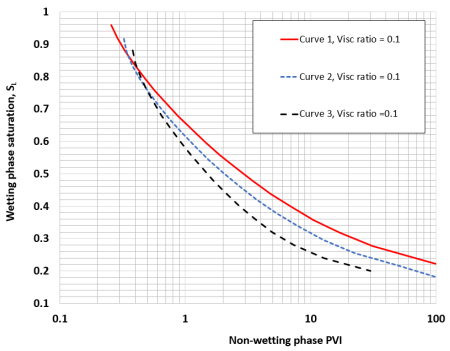

Fig. 10. Wetting phase saturation as a function of PVI, using relative permeabilities in Figure 7 with viscosity ratio of 0.1.

3.2 Integrated uncertainty-based workflow

In the system under investigation, characterized by high IFT, conventional sandstone within a limited range of porosity and permeability, low capillary numbers and strong water-wet conditions, we anticipate that the relative permeabilities and associated mobilities will be confined to a certain range. Selecting samples with satisfying rock properties would address geological uncertainties to a certain extent, particularly those related to porosity and permeability.

Under the uncertainty framework, we estimate three sets of relative permeability that yield low, medium, and high injectivity. Total mobility is a good proxy to rank the set. We identify low, medium, and high cases for the total mobility and displacement curves to represent the effect of any given set of relative permeability on the modeling of injectivity. Plots in Figure 11 and Figure 12 illustrate the total mobility and displacement curves, respectively, for the sets of relative permeability shown in Figure 3.

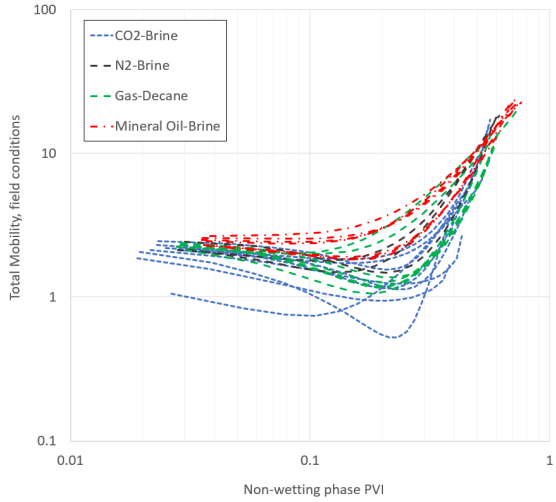

Fig. 11. Total mobility as a function of non-wetting phase saturation (injected phase). Total mobility is calculated using relative permeability in Figure 3 with viscosity ratio of 0.1.

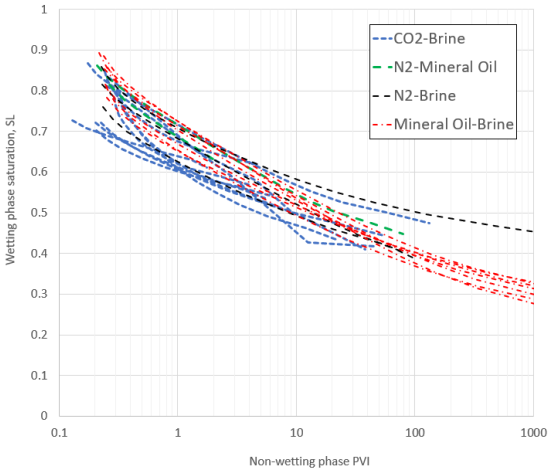

Fig. 12. Wetting phase saturation as a function of PVI, using relative permeabilities in Figure 3 with viscosity ratio of 0.1.

Figure 11 displays the effect of the wide range of uncertainty in the wetting phase for the CO_2/brine pair for the lower values of non-wetting saturation, which may be likely caused by experimental artifacts. We also see some trend towards lower injectivity for the CO_2/brine.

Considering the uncertainties in these measurements and the trends observed in Figure 11 and Figure 12, CO_2/brine can be approximated by using gas/mineral oil or N_2/brine if measurements are not available, weighting towards low values for the non-wetting phase. This finding enables us to use conventional drainage N_2/mineral oil measurements, routinely measured for oil and N_2 projects, from analog fields. The wetting phase uncertainty window can be narrowed somewhat by narrowing the range using this method, which accounts for both geologic and process uncertainty.

Based on the range of data and trends in Figure 11 and Figure 12 as guides, we estimate three sets of relative permeability that yield low, mid, and high case scenarios for injectivity. Figure 13 shows the sets estimated for this study, with the corresponding total mobilities and

displacement plot in Figure 14 and Figure 15, respectively.

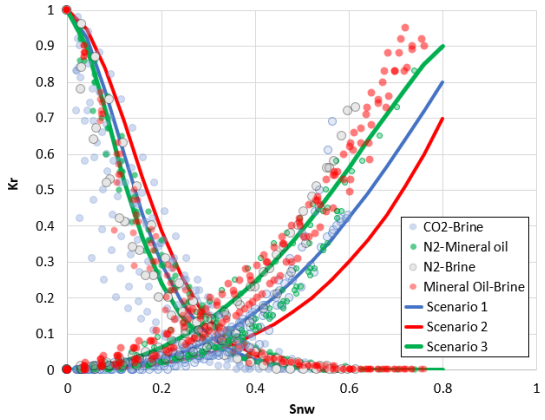

Fig. 13. Relative permeabilities as shown in Figure 3 (symbols) with sets of relative permeabilities corresponding to three scenarios in Figure 14 and Figure 15.

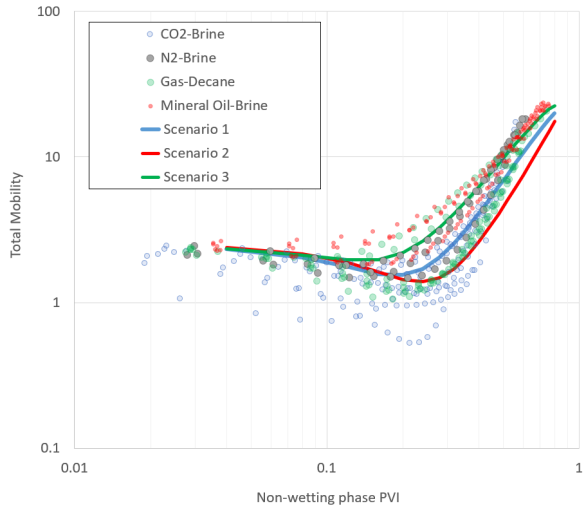

Fig. 14. Total mobility as a function of non-wetting phase pore volumes injected). Data in Figure 11 is shown as symbols and the three scenarios obtained from sets shown in Figure 13.

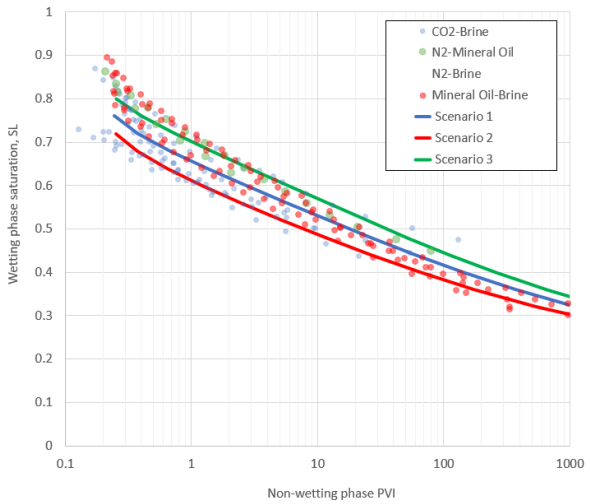

Fig. 15. Wetting phase saturation as a function of PVI. Data in Figure 12 is shown as symbols and the three scenarios obtained from sets shown in Figure 13.

4. Use of analogs

Measurements of drainage relative permeability using nitrogen/mineral oil pair are routinely performed as they are part of most core analysis programs in oil and N_2 operations. To show the application of this data in CCUS studies, we chose nitrogen/mineral oil measurements in a target field with similar properties to those studies in the previous sessions.

Figure 16 and Figure 17 show the total mobility and wetting phase saturation as a function of PVI shown in Figure 11 and Figure 12, respectively, when adding results using nitrogen/mineral oil relative permeability measurements in analog samples from our target field. Both figures show good agreement in the uncertainty range. This uncertainty range goes through the same analysis to derive low/mid/high CO_2/brine relative permeabilities.

Figure 18 compares the typical range of viscosity ratio and IFT for nitrogen/mineral oil with the data analyzed in this work. The fact that we are in the region close to the middle of the range together with the capturing of rock with relatively similar rock properties, explains in good part the agreement in the uncertainty band.

The nitrogen/mineral oil drainage relative permeability measurements are generally performed in samples with connate water saturation, which will result in a final state with liquid saturations (i.e., $S_{wc}+S_{org}$) higher than what we expect in the CO_2 injection, and as in the case of previous session, plot in Figure 12 is valuable in extrapolating endpoint to target minimum water saturation endpoint.

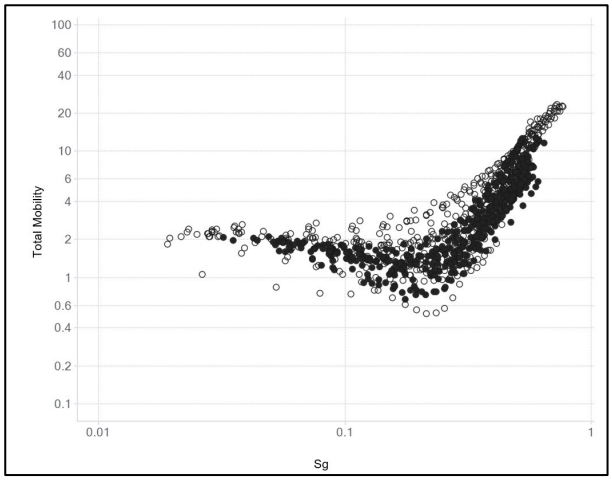

Fig. 16. Comparison of total mobility as a function of non-wetting phase pore volumes injected (injected phase) obtained for previous session with different fluid pairs (Figure 11) as white circles and field analog nitrogen/mineral oil data used for this example (dark symbol).

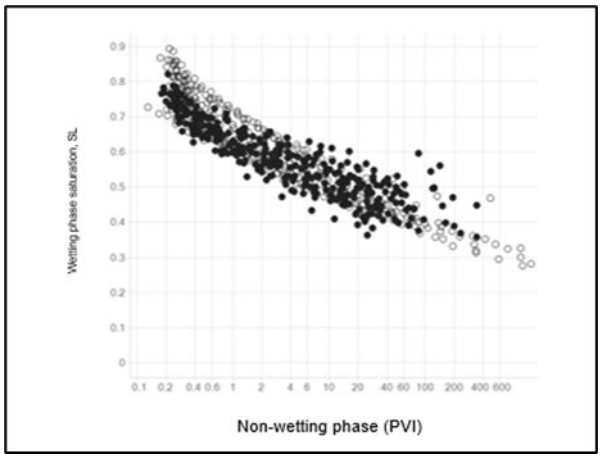

Fig. 17. Comparison of wetting phase saturation as a function of PVI, obtained with different fluid pairs in previous session (Figure 12) shown by white circles and field analog nitrogen/data used in this example shown as dark symbols.

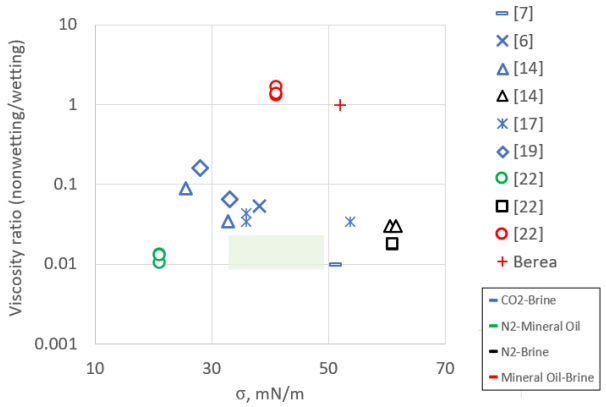

Fig. 18. Viscosity ratio and IFT ranges considered in this study compared with ranges typical of nitrogen/mineral oil used in routine measurements (Green square).

5. Recommendations

Based on the observations made in this study, here are some recommendations for ongoing and future work:

<u>In cases where CO_2/brine data is not available:</u>

- Check for ranges of viscosity ratio and IFT covered during the injection / storage process to validate use of analog fluids.
- Use of N_2/mineral oil and/or N_2/brine relative permeability in analog fields within porosity, permeability, and clay composition range.
- The assessment of minimum water saturation reached during injection should be done by looking at porous plate and centrifuge data, and the endpoint of N_2 relative permeability should be estimated by using combination of fractional flow plots with total mobility (Figure 11 and Figure 12).
- When estimating relative permeability, we may need to consider that N_2/mineral oil could be on the optimistic side and adjust for it.

<u>In cases where CO_2/brine studies are planned:</u>

Recommend planning for two sub-sets of tests:

- Measurements to probe the geological uncertainties consists of measurements of N2/mineral oil and /or N2/brine endpoints at multiple flow rates. These endpoints, together with capillary pressure are used as guardrails during the methodology described in the previous section and help simulation engineers with decisions about binning based on grid properties.
- Measurements to probe the process uncertainty consist of:
  - Seventy percent (70%) of efforts focused on complete N_2/mineral oil or N_2/brine relative permeability.
  - Additional percentage (30%) of efforts focus on CO_2/brine Steady-State relative permeability tests. Follow with Unsteady State endpoints after the CO_2/brine Steady State measurements are completed.

6. Conclusions

The scarcity and inconsistency of experimental data on CO_2/brine drainage relative permeability, due to the nature and complications of these experiments, limits our understanding of the relative permeability for a broad range of saturations and challenges the effective representation of the injection mechanisms for the CCS projects.

In this study, we compared various fluid pair systems in a limited set of sandstone rocks published in the literature and analyzed the data under the lenses of total mobility and displacement efficiency. The workflow allows for analysis of different fluid systems compared to CO_2/brine and gauge effects of the various source of uncertainty.

Our findings indicate that while we can use nitrogen/mineral oil and/or nitrogen/brine testing as analog for these measurements, the slightly lower total mobility exhibited by CO_2/brine pair can be a concern. We recommend, whenever feasible, to perform some limited experiments with CO_2/brine in the low saturation range and complete the relative permeability saturation range with analog fluids.

Nomenclature

CCI: counter-current imbibition test.
CCUS: Carbon Utilization and Storage.
f: fractional flow, as defined in eq. 4.
IFT: Interfacial tension, also known as σ.
k_r: relative permeability.
N_c: Capillary number, as defined in eq. 1.
PVI: pore volume injected.
S: saturation,
u: speed of advance,
λ: mobility, as defined in eq. 3
μ: viscosity
σ: interfacial tension, also written as IFT.

Subscripts
L: liquid
nw: non-wetting phase
w: wetting phase
p_n: phase *n*.
t = total, both phases, in the context of mobility, eq. 2
L=liquid

References

1. D. B. Bennion and S. Bachu. Relative permeability characteristics for supercritical CO_2 displacing water in a variety of potential sequestration zones in the western Canada sedimentary basin. In SPE Annual Technical Conference and Exhibition, SPE-95547 (2005).
2. D. B. Bennion and S. Bachu. Dependence on temperature, pressure, and salinity of the IFT and relative permeability displacement characteristics of CO_2 injected in deep saline aquifers. In SPE Annual Technical Conference and Exhibition, SPE-102138. (2006).
3. D. B. Bennion and S. Bachu. Drainage and imbibition relative permeability relationships for supercritical CO_2/brine and H_2S/brine systems in intergranular sandstone, carbonate, shale, and anhydrite rocks. SPE Reservoir Evaluation & Engineering 11 (3): 487-496 (2008).
4. S. Bachu and B. Bennion. Effects of in-situ conditions on relative permeability characteristics of CO_2-brine systems. Environmental Geology 54: 1707-1722 (2008).
5. J. C. Perrin, M. Krause, C.W. Kuo, L. Miljkovic, E. Charoba, and S. M. Benson. Core-scale experimental study of relative permeability properties of CO_2 and brine in reservoir rocks. Energy Procedia 1, (1): 3515-3522 (2009).
6. J.C. Perrin and S. Benson. An experimental study on the influence of sub-core scale heterogeneities on CO_2 distribution in reservoir rocks. Transport in porous media 82: 93-109 (2010).
7. M. Akbarabadi, and M. Piri. Relative permeability hysteresis and capillary trapping characteristics of supercritical CO_2/brine systems: An experimental study at reservoir conditions. Advances in Water Resources 52: 190-206 (2013).
8. S. Benson, R. Pini, C. Reynolds, and S. Krevor. Relative permeability analyses to describe multi-phase flow in CO_2 storage reservoirs. Global CCS Institute (2013).
9. J. S. Levine, D. S. Goldberg, K. S. Lackner, J. M. Matter, M. G. Supp, and T. S. Ramakrishnan. Relative permeability experiments of carbon dioxide displacing brine and their implications for carbon sequestration. Environmental science & technology 48 (1): 811-818 (2014).
10. C. R. Reynolds, M. Blunt and S. Krevor, Impact of reservoir conditions on CO_2-brine relative permeability in sandstones. Energy Procedia 63: 5577-5585 (2014).
11. C. Ruprecht, R. Pini, R. Falta, S. Benson, and L. Murdoch. Hysteretic trapping and relative permeability of CO_2 in sandstone at reservoir conditions. International Journal of Greenhouse Gas Control 27: 15-27 (2014).
12. C. R. Reynolds and S. Krevor, Characterizing Flow Behavior for Gas Injection: Relative Permeability of CO_2-Brine and N_2-Water in Heterogeneous Rocks, Water Resources Research, 51(12): 9464– 9489 (2015).
13. X. Chen and D. A. DiCarlo. A new unsteady-state method of determining two-phase relative permeability illustrated by CO_2-brine primary drainage in Berea sandstone. Advances in Water Resources 96: 251-265 (2016).
14. P. B. Jordan, Two-phase relative permeability measurements in Berea sandstone at reservoir conditions. PhD diss. (2016).
15. X. Chen, S. Gao, A. Kianinejad, and D. A. DiCarlo. Steady-state supercritical CO_2 and brine relative permeability in Berea sandstone at different temperature and pressure conditions. Water Resources Research (53): 6312-6321 (2017).
16. S. A. Smith, C. J. Beddoe, B. A. Mibeck, L.V. Heebink, B. A. Kurz, W. D. Peck, and L. Jin. Relative permeability of Williston Basin CO_2 storage targets. Energy Procedia 114: 2957-2971 (2017).
17. G. S. Jeong, S. Ki, D. S. Lee, and I. Jang. Effect of the flow rate on the relative permeability curve in the CO_2 and brine system for CO_2 sequestration. Sustainability 13 (3):1543 (2021).
18. E. Ebeltoft, M. Recordon, R. Meneguolo, J. Gausdal Jacobsen, R. Askarinezhad, and R. Pitman. SCAL model for CCS-insights from the first commercial CO_2 project on the norwegian continental shell, northern lights. In Proceedings of the International Symposium of the Society of Core Analysts, 2023-16 (2023).
19. B. Gao, E. Lyons, D. Magzymov, L. Poore, G. Besil, S. Richardson, and L. Lun. Steady-state supercritical CO2 and brine relative permeability measurements at different pressure conditions, In Proceedings of the International Symposium of the Society of Core Analysts, 2023-15 (2023).
20. M. Mascle, A. Oisel, P. K. Munkerud, E. Ebeltoft, O. Lopez, C. Pryme, and S. Youssef. C_{O2}-Brine Relative Permeability Measurements at Reservoir Conditions: how to reconciliate SS and USS methods? In Proceedings of the International Symposium of the Society of Core Analysts, SCA 2023-002 (2023).
21. L. Tang, G. Ding, S. Song, H. Wang, W. Xie, Y. Zhou, Z. Song, C. Xie, and H. Song. Effect of Confining Pressure on CO2-Brine Relative Permeability Characteristics of Sandstone in Ordos Basin. Water 15 (24):4235 (2023).

22. M. J. Oak, Three-phase relative permeability of water-wet Berea. In SPE Improved Oil Recovery Conference, SPE-20183 (1990).
23. M. J. Oak, L. E. Baker, and D. C. Thomas. Three-phase relative permeability of Berea sandstone. Journal of Petroleum Technology 42 (8): 1054-1061 (1990).
24. L. E. Baker, Three-phase relative permeability of water-wet, intermediate-wet, and oil-wet sandstone. Geological Society, London, Special Publications 84 (1): 51-61 (1995).
25. D. A. DiCarlo, A. Sahni, and M. J. Blunt, Three-phase relative permeability of water-wet, oil-wet, and mixed-wet sandpacks. SPE Journal 5 (1): 82-91 (2000).
26. Y. Cinar and F. M. Orr. Measurement of three-phase relative permeability with IFT variation." SPE Reservoir Evaluation & Engineering 8 (1): 33-43 (2005).
27. P. Cao and S. Siddiqui. Three-phase unsteady-state relative permeability measurements in consolidated cores using three immiscible liquids. In SPE Annual Technical Conference and Exhibition, SPE-145808. (2011).
28. A. H. Alizadeh and M. Piri, The effect of saturation history on three-phase relative permeability: An experimental study. Water Resources Research, 50(2): 1636-1664. (2014).
29. J. Kamath, F. Nakagawa, J. Schembre, T. Fate, E. DeZabala, and P. Ayyalasomayajula, Core Based Perspective on Uncertainty in Relative Permeability. In Proceedings of the International Symposium of the Society of Core Analysts, 2005-30 (2005).
30. J. M. Schembre-McCabe, J. Kamath and R. Gurton. Mechanistic studies of CO_2 sequestration. In International Petroleum Technology Conference, European Association of Geoscientists & Engineers, (2007).
31. S. C. M. Krevor, R. Pini, L. Zuo, and S. M. Benson, Relative permeability and trapping of CO2 and water in sandstone rocks at reservoir conditions, Water Resources Research, (48) 2, (2012).
32. J. Kokkedee, W. Boom, A. Frens, and J. Maas, Improved Special Core Analysis: Scope for a reduced residual oil saturation, In Proceedings of the International Symposium of the Society of Core Analysts, SCA 1996-01 (1996).
33. P. G. Saffman and G. I. Taylor. The penetration of a fluid into a porous medium or Hele-Shaw cell containing a more viscous liquid. Proceedings of the Royal Society of London. Series A. Mathematical and Physical Sciences 245, (1242): 312-329 (1958).
34. S. E. Buckley and M. Leverett. Mechanism of fluid displacement in sands. Transactions of the AIME 146 (1): 107-116 (1942).
35. L. P. Dake, Fundamentals of Reservoir Engineering, Elsevier (1983).
36. N. Suwandi, F. Jiang, and T. Tsuji, Relative permeability variation depending on viscosity ratio and capillary number. Water Resources Research 58(6) (2022).
37. G. Sun, Z. Sun, A. Fager, and B. Crouse. Pore-scale Analysis of CO2-brine Displacement in Berea Sandstone and Its Implications to CO2 Injectivity. In E3S Web of Conferences, EDP Sciences, 367, p. 01011 (2023).